






## RESEARCH ARTICLE

# Topography modulates climate sensitivity of multidecadal trends of holm oak decline

Ana López-Ballesteros<sup>1</sup>  | Emilio Rodríguez-Caballero<sup>2</sup>  | Gerardo Moreno<sup>3</sup>  |  
Paula Escribano<sup>4</sup> | Ana-Maria Hereş<sup>5,6</sup>  | Jorge Curiel Yuste<sup>6,7</sup> 

<sup>1</sup>Department of Agricultural and Forest Systems, and the Environment, Agrifood Research and Technology Centre of Aragon (CITA), Zaragoza, Spain

<sup>2</sup>Department of Agronomy and Centro de Investigación de Colecciones Científicas (CECOUAL), Universidad de Almería, Almería, Spain

<sup>3</sup>Forestry School, Institute for Dehesa Research (INDEHESA), Universidad de Extremadura, Plasencia, Spain

<sup>4</sup>Biodiversity Node S.L., Madrid, Spain

<sup>5</sup>Faculty of Silviculture and Forest Engineering, Transilvania University of Braşov, Braşov, Romania

<sup>6</sup>BC3—Basque Centre for Climate Change, Scientific Campus of the University of the Basque Country, Leioa, Spain

<sup>7</sup>IKERBASQUE, Basque Foundation for Science, Bilbao, Spain

## Correspondence

Ana López-Ballesteros, Department of Agricultural and Forest Systems, and the Environment, Agrifood Research and Technology Centre of Aragon (CITA), Avda. Montañana 930, 50059 Zaragoza, Spain.

Email: [alpzballesteros@gmail.com](mailto:alpzballesteros@gmail.com)

## Funding information

Agencia de Innovación y Desarrollo de Andalucía; Ministerio de Ciencia e Innovación; Ministerul Cercetării și Inovării

## Abstract

Forest decline events have increased worldwide over the last decades being holm oak (*Quercus ilex* L.) one of the tree species with the most worrying trends across Europe. Since this is one of the tree species with the southernmost distribution within the European continent, its vulnerability to climate change is a phenomenon of enormous ecological importance. Previous research identified drought and soil pathogens as the main causes behind holm oak decline. However, despite tree health loss is a multifactorial phenomenon where abiotic and biotic factors interact in time and space, there are some abiotic factors whose influence has been commonly overlooked. Here, we evaluate how land use (forests versus savannas), topography, and climate extremes jointly determine the spatiotemporal patterns of holm oak defoliation trends over almost three decades (1987–2014) in Spain, where holm oak represents the 25% of the national forested area. We found an increasing defoliation trend in 119 out of the total 134 holm oak plots evaluated, being this defoliation trend significantly higher in forests compared with savannas. Moreover, we have detected that the interaction between topography (which covariates with the land use) and summer precipitation anomalies explains trends of holm oak decline across the Mediterranean region. While a higher occurrence of dry summers increases defoliation trends in steeper terrains where forests dominate, an inverse relationship was found in flatter terrains where savannas are mainly located. These opposite relationships suggest different causal mechanisms behind decline. Whereas hydric stress is likely to occur in steeper terrains where soil water holding capacity is limited, soil waterlogging usually occurs in flatter terrains what increases tree vulnerability to soil pathogens. Our results contribute to the growing evidence of the influence of local topography on forest resilience and could assist in the identification of potential tree decline hotspots and its main causes over the Mediterranean region.

## KEYWORDS

climate change, climatic anomalies, coppices, defoliation, dehesas, Mediterranean forest, tree health

## 1 | INTRODUCTION

The number of tree mortality and forest decline events have increased worldwide over the last decades (Allen et al., 2015; Hammond et al., 2022), with accelerating rates being associated with climate change (McDowell et al., 2022; Parmesan et al., 2022). These decline patterns have global implications in the current climate change context as they negatively affect the global land carbon sink (Clark et al., 2010; Haberstroh et al., 2022; Liu et al., 2023) as well as soil functioning and diversity (Curiel Yuste et al., 2019; García-Angulo et al., 2020; Rodríguez et al., 2017). Although the primary physiological mechanisms behind tree mortality are related to water and heat stress (Allen et al., 2010, 2015), climate extremes can also amplify the occurrence and impact of other disturbance drivers, such as wildfires and pathogen outbreaks (Brando et al., 2014; Gea-Izquierdo et al., 2021; Seidl et al., 2017). Regional studies based on either systematic forest inventories or remote sensing observations have identified the Mediterranean basin as a hotspot of forest decline (Carnicer et al., 2011; Forest, 2020; Senf et al., 2020). This has coincided with an increase in the magnitude and frequency of heat waves and droughts since the preindustrial era (Douville et al., 2021; Markonis et al., 2021; Seneviratne et al., 2021; Vicente-Serrano et al., 2014). Foreseeably, the higher occurrence probability of longer and more severe droughts projected across the Mediterranean region (García-Valdecasas Ojeda et al., 2021) will pose an even higher mortality risk to Mediterranean tree species in the near future.

One of these tree species that has already shown clear signs of decline is *Quercus ilex* L. (hereinafter holm oak). Holm oak is one of the most representative species of southern Europe, which naturally grows in areas with Mediterranean climate characterized by summer drought periods and cold or mild moist winters (Lionello et al., 2006), expanding over 18 European and African countries (Caudullo et al., 2017). However, it is also present in areas of temperate climate as an introduced tree species. This species occurs over a large range of altitudes, from sea level up to 2500 m.a.s.l. (Barbero et al., 1992), given its ability to cope with drought and heat stress by means of stomatal regulation and photoprotective mechanisms (Alonso-Forn et al., 2021; Sancho-Knapik et al., 2022). However, acute signs of holm oak decline have been detected across the Iberian Peninsula, including growth reduction (Corcuera et al., 2004; Gea-Izquierdo et al., 2011; Hereş et al., 2018), partial crown defoliation (Carnicer et al., 2011; Forest Europe, 2020), branch dieback, and tree death (Lloret et al., 2004; Sánchez-Cuesta et al., 2021). In fact, Europe-wide defoliation surveys have identified evergreen oaks as the species group with the highest increase in defoliation over the last 20 years (Michel et al., 2021). These declining symptoms have been detected in both major land uses where Mediterranean holm oak woodlands dominate across southern Europe (Gazol et al., 2020). These land uses show contrasted structure and correspond to dense forests traditionally managed as coppices (hereafter forest; Giovannini et al., 1992) and human-made savanna-like ecosystems—named as “dehesas” or “montados” in Spain and Portugal, respectively—which are managed as silvopastures with a far less tree density that

allow for the extensive livestock rearing (hereafter savanna; Moreno & Rolo, 2019; Plieninger et al., 2015; Pulido et al., 2001). The geographical distribution of these land-use types is generally determined by local topography. While savannas occupy topographically smooth areas, coppice forests are largely found in topographically complex areas with steeper slopes. Understanding the causes of holm oak decline at both forest- and savanna-like ecosystems remains a scientific priority to preserve the valuable socio-ecological services that these habitats have provided for centuries (Gil-Pelegrín et al., 2017; Plieninger et al., 2015; Sáez et al., 2007; Stavi et al., 2022; Terradas, 1999).

Previous research suggests different prevailing mechanisms behind holm oak decline in these land-use types. On one hand, decline episodes in holm oak forests have been associated with carbon starvation (Galiano et al., 2012) and drought-induced xylem embolism, which reduces the water uptake capacity of the trees leading to leaf desiccation, and shoot, branch, or tree mortality (Barbeta et al., 2013; Corcuera et al., 2004; Lloret et al., 2004). Furthermore, the abandonment of the traditional coppicing practices derived from rural depopulation (López et al., 2009; Serrada et al., 1992) has shaped the structure of these forests into stands with a higher density of overaged individuals with aggravated water stress and drought vulnerability (Gazol et al., 2020; Moreno & Cubera, 2008; Rodríguez-Calcerrada et al., 2011). On the other hand, holm oak decline in Mediterranean savannas has been primarily associated with soil-borne pathogen outbreaks of *Phytophthora cinnamomi* Rands (hereinafter *Phytophthora* spp.; Brasier et al., 1993), which causes hydraulic failure through root damage, and triggers similar decline symptoms to the drought-induced ones (Corcobado et al., 2014; de Sampaio e Paiva Camilo-Alves et al., 2013; Encinas-Valero, Esteban, Hereş, María Becerril, et al., 2022). Recent evidence indicates that defoliation patterns in savannas may also be caused by changes in the shot-to-root nonstructural carbon allocation patterns associated with the belowground stress caused by this pathogen (Encinas-Valero, Esteban, Hereş, Vivas, et al., 2022). However, there is no consensus on how pathogenicity and climate stress interact. While some studies state that pathogenicity can be presumably amplified by climatic stress (Brasier, 1996; González et al., 2020; Rodríguez-Molina et al., 2005), others suggest that drought reduces the risk of pathogen damage (Homet et al., 2019; Serrano et al., 2022).

These contrasting results reveal that holm oak health loss and mortality is a multifactorial phenomenon where abiotic and biotic factors interact in time and space (Brando et al., 2014; Gea-Izquierdo et al., 2021; Seidl et al., 2017), but not all factors potentially involved have been equally evaluated. It has been demonstrated that land use (i.e., forest structure and management) can modulate the effect of climate on forest dieback/die-off/mortality (Alfaro-Sánchez et al., 2019; Gentilella et al., 2017; Sangüesa-Barreda et al., 2015). Still, very few studies have assessed the role of this factor in holm oak decline (e.g., Gazol et al., 2020). Likewise, previous research has shown that local topography influences how forest resilience (Carnicer et al., 2021), phenology (Adams et al., 2021), and decline (Wang et al., 2021) respond to climate variability. In this sense, topographic

features together with vegetation structure strongly determine local microclimate (Bennie et al., 2008; Bramer et al., 2018; Ma et al., 2010; Scherrer & Körner, 2010) and soil water availability (Burt & Butcher, 1985; Huang et al., 2012; Tromp-van Meerveld & McDonnell, 2006). Despite the complex topography of the Mediterranean region, there is a lack of regional studies where systematic observations of holm oak decline cover areas with topographic and climate variability and where both holm oak forests and savannas are represented.

In this study, our general aim is to better understand the phenomenon of holm oak decline, given its socio-ecological and economic relevance in the Mediterranean basin and especially in Spain, where holm oak represents 25% of the forested area and 16% of wood production (Terradas, 1999). Thus, we have made use of public databases to evaluate how land use, topography, and climate extremes jointly relate to spatiotemporal patterns of holm oak defoliation over almost three decades (1987–2014) in Spain. We have geographically framed our study in the Spanish territory as this is the southern edge of forest distribution in the European continent, it covers a wide variety of topographic characteristics, and it also covers the entire spectrum of ecological niches of this tree species (Martín-Sánchez et al., 2022). We hypothesize that both land use and associated topographic features determine the vulnerability of holm oak to climate variability and extremes, resulting in different climate-decline relationships in holm oak-dominated ecosystems. Our specific objectives are (i) to compare multidecadal trends of holm oak defoliation between the main land-use types (i.e., forests vs. savannas); and (ii) to disentangle the interactive influence of land use, local topography, and climate anomalies on multidecadal trends of holm oak defoliation.

## 2 | MATERIALS AND METHODS

### 2.1 | Data sources and processing

Several public datasets were utilized to investigate the influence of land use, climate, and topography on holm oak defoliation across Spain over the period 1987–2014. Main specifications of these geo-spatial and survey datasets are summarized in Table S1.

#### 2.1.1 | Defoliation data

The annual holm oak crown defoliation data used in this study span from 1987 to 2014 and were obtained from the survey data of the Level 1 network of the International Co-operative Programme on Assessment and Monitoring of Air Pollution Effects on Forests (ICP Forests; Eichhorn et al., 2016). Starting from 1987, the Level I monitoring scheme of ICP Forests annually surveys crown defoliation at >5000 forested plots, which are systematically arranged in a nominal 16 × 16 km grid throughout Europe. For this study, we only used plots where holm oak was present and a minimum number of three

observations every 7-year period were available over the whole 28-year study period (1987–2014). This filtering criteria yielded a total of 134 plots spread across the entire holm oak distribution area in Spain (Figure 1) with data spanning from 24 to 28 years surveyed. These circular plots of 50-m radius contained at least one predominant, dominant, and co-dominant holm oak tree (i.e., minimum height of 60 cm) that showed no significant mechanical damage (Eichhorn et al., 2016). From the total of 134 plots analyzed in this study, 90% of them included at least five holm oak trees per plot. Tree crown defoliation was visually evaluated, always during the summer season, by associating a percentage of leaf loss in the assessable crown as compared to a reference tree, using a sliding scale of 5%. Reference trees were defined as trees with the best full crown foliage that could grow at each plot.

#### 2.1.2 | Land-use data

The land use of each of the selected ICP plots was derived from the 2014 version (last version available) of the SIOSE (Land Cover and Land Use Information System of Spain) database (1:25,000; Equipo Técnico Nacional SIOSE, 2015; Equipo Técnico Nacional SIOSE, 2015). We extracted the codes of those land-use polygons that overlapped the centroids of each of the 134 ICP holm oak plots. Land-use codes provide information of the cover types present in each polygon together with their respective coverage area over the total polygon area. Based on this information, we defined two different land-use classes, forest (F) and savanna (S). Concretely, when conifer, deciduous, and/or evergreen broadleaf forests occupied at least 50% of the polygon, the overlapping ICP plot was defined as

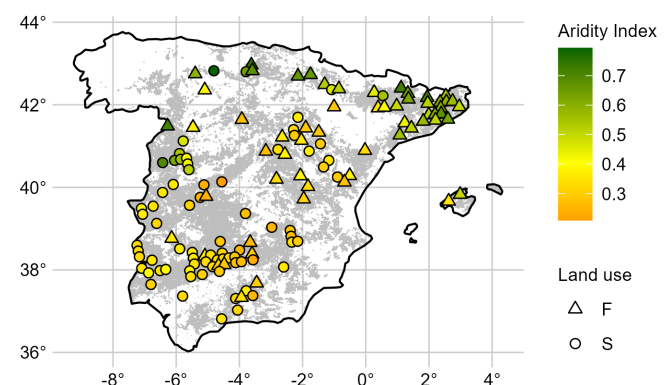


**FIGURE 1** Location of the 134 ICP holm oak plots over the distribution area of holm oak in Spain (gray area). Circles and triangles represent savanna (S) and forest (F) plots, respectively, while their colors indicate the annual averaged plot-mean aridity index (AI) over the 1970–2000 period with green and orange colors indicating less (close to 1) and more (close to 0) arid areas. This plot-mean AI was extracted from the Global Aridity Index and Potential Evapo-Transpiration (ET<sup>p</sup>) Climate Database v2 (Trabucco & Zomer, 2019). The holm oak distribution map was provided by GIS-FOREST INIA (Ministerio de Medio Ambiente, y medio Rural y Marino, 2009). [Colour figure can be viewed at [wileyonlinelibrary.com](https://onlinelibrary.wiley.com)]

a forest, otherwise, it was defined as a savanna. To do so, we used the *sf* (Pebesma, 2018) R package and Google Earth Pro (version 7.3.6.9285) to visually double-check assigned land-use classes.

### 2.1.3 | Climatic data

Two different databases were utilized to collate climatic data for the ICP holm oak plots utilized in this study. First, the annual average of the aridity index (AI) over the 1970–2000 period was extracted from the Global Aridity Index and Potential Evapo-Transpiration (ETO) Climate Database v2 (1-km spatial resolution; Trabucco & Zomer, 2019). Second, seasonal maximum, minimum, and mean air temperature together with precipitation values were obtained from the Spain02 v5.0 gridded datasets (10-km spatial resolution; Herrera et al., 2012, 2016). Seasonal climatic anomalies (MAM for spring, JJA for summer, SON for autumn, and DJF for winter) were calculated by subtracting the averaged seasonal value over the whole study period (1987–2014) to the seasonally averaged value of each year. Hence, negative anomalies correspond to seasons when temperature and/or precipitation were lower than the historical average, while positive anomalies correspond to seasons when the opposite occurred, that is, temperature and/or precipitation were higher than the historical average. Anomaly units were degrees Celsius for temperature and mm for precipitation. As defoliation surveys were annually performed during the summer season, the summer and autumn climatic datasets of the same years when defoliation was measured were excluded from the correlation analysis. Thus, five seasons were analyzed, from spring of the previous year to spring of the current year when defoliation measurements were collected. All these data processing steps were performed by using the *lubridate* (Grolemund & Wickham, 2011), *ncdf4* (Pierce, 2019), *raster* (Hijmans, 2021), *sf* (Pebesma, 2018), and *tidyverse* (Wickham et al., 2019) R packages.

### 2.1.4 | Topographic data

Mean and variance values of several topographic variables were obtained for the ICP holm oak plots to consider the averaged geomorphology of the surface together with its complexity. Slope and altitude values were extracted from a 5-m digital elevation model (DEM) obtained from the LIDAR flights 1st Coverage of the National Plan for Aerial orthophotography (PNOA; Spanish Geographic Information National Center, CNIG). Mean aspect was derived from the DEM tiles and reclassified into eight groups by using 45-degree intervals spanning from north to northwest directions. Terrain curvature parameters and topographic wetness index (TWI) were also derived from the DEM tiles to consider plot-surface water flow dynamics. Concretely, profile curvature represents the acceleration of the water flow in the slope direction with positive values associated with upwardly convex surface and negative values to upwardly concave surface for a specific grid cell (Florinsky, 2000). The planform curvature represents the convergence of the water flow in the

maximum slope-perpendicular direction with negative and positive values representing sidewardly concave and convex surfaces, respectively, while zero values representing linear surface. The TWI quantifies the terrain-driven variation in soil moisture by integrating the water supply from the upslope catchment area and the slope gradient for each grid cell in a DEM (Kopecký et al., 2021). To get plot-scale TWI estimates, a sink removal algorithm with a minimum slope threshold of 0.01 degrees was first applied to fill the sinks in the DEM tiles prior to calculation of the upslope accumulated area according to the triangular multiple flow direction algorithm (Seibert & McGlynn, 2007). Then, the specific catchment area (SCA; m) was computed via the multiple flow direction algorithm (Quinn et al., 1991) and utilized to get the TWI (dimensionless) according to Beven and Kirkby (1979), as follows:

$$TWI = \ln \frac{SCA}{\tan(\text{slope})}$$

Prior to the extraction of zonal statistics, each raster file was reclassified to assure that the values of each topographic variable were within plausible ranges (see Table S2). All the DEM-derived variables were computed for each tile and subsequently extracted for each ICP plot by using the *exactextractr* (Baston, 2022), *RSAGA* (Brenning et al., 2018), *raster* (Hijmans, 2021), and *sf* (Pebesma, 2018) R packages.

## 2.2 | Statistical analyses

The complete analyses workflow followed in this study are depicted in Figure 2. First, mean defoliation per plot and year was calculated. Afterward, multidecadal defoliation trends for each ICP holm oak plot were computed as the Sen's slope regression coefficient (Sen, 1968) between year and annual defoliation values by using the *trend* R package (Pohlert, 2020). We used Sen's slope as this nonparametric estimate has been proven more robust for observational data compared with linear regression. Mean and trend values of defoliation over the study period (1987–2014) were then compared between forest (F) and savanna (S) land uses by using them as explanatory variables in either ANOVA or Kruskal–Wallis tests after checking the normality assumption of the data distribution via a Shapiro normality test and graphic representation. Eta squared ( $\eta^2$ ) was computed by means of the *rstatix* R package (Kassambara, 2022) to provide an estimate of how much variance in the response variable is explained by the explanatory variable.

Multiple linear regression models were used to explore potential links between abiotic factors (climate, topography, and land use) and defoliation trends. Prior to modeling, we performed principal component analysis (PCA) to reduce the dimensionality of the topographic characterization data from each plot via the *factoextra* R package (Kassambara & Mundt, 2020). Variables considered in the PCA corresponded to mean and variance values of altitude, slope, profile and planform curvature, topographic wetness index (TWI), and reclassified mean aspect (i.e., 11 topographic variables). Moreover, seasonal climate anomalies were temporally aggregated

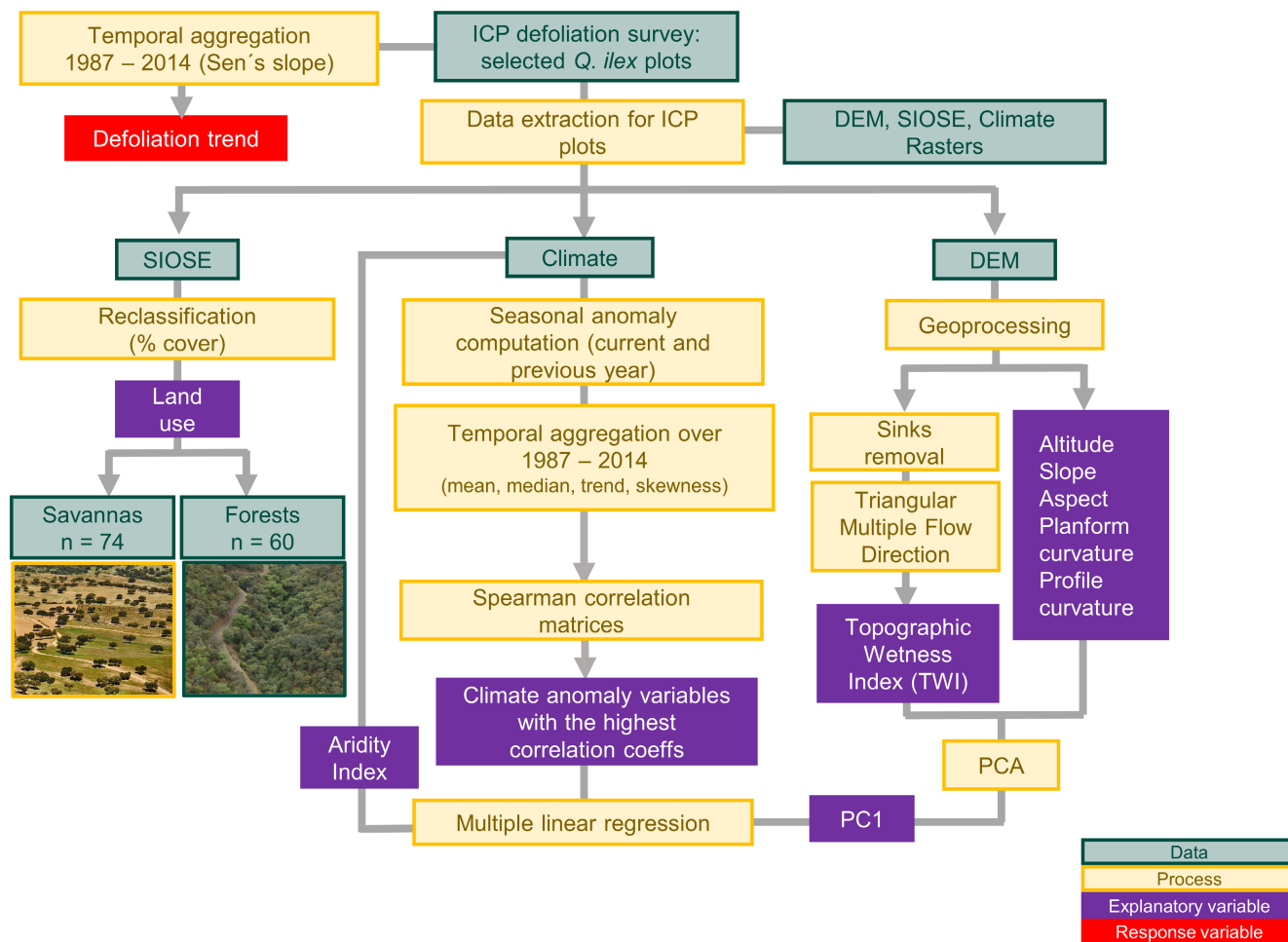


**FIGURE 2** Diagram summarizing the methodological and statistical workflow followed in this study. [Colour figure can be viewed at [wileyonlinelibrary.com](https://onlinelibrary.wiley.com/doi/10.1111/gcb.16927)]

by computing their mean, median, skewness, and Sen's slope values over the study period (1987–2014). Then, Spearman correlation matrices among aggregated climatic anomalies and between these and defoliation trends were computed to select those climatic variables to be included in the defoliation model while avoiding multicollinearity. The Spearman coefficients, together with their associated p-values, were calculated by using the Hmisc R package (Harrell, 2021). The defoliation model was built via multiple linear regression. The defoliation Sen's slopes were set as the response variable, while explanatory variables of the full model corresponded to the topographic features synthesized via PCA, the previously selected aggregated seasonal climate anomalies, the interactions among them, and the aridity index (Figure 2). We were especially interested in the topography–climate interactions as a way to indirectly include microclimate effects in our model. Besides, we included the aridity index (AI) as a way to include in our model the general climatic characteristics of our ICP plots. All these explanatory variables were scaled prior to modeling. Model selection was performed by using the backward and forward stepwise Akaike's information criterion (AIC) algorithm (Venables & Ripley, 2002). The residuals of the final model fulfilled the normality and heteroskedasticity assumptions. Spatial autocorrelation was checked by means of the Moran's I test

for distance-based autocorrelation (Moran, 1950). In order to explore the potential role of stand age in the defoliation trends, the same workflow was applied to a subset of ICP plots where a specific mean stand age at plot scale was provided. This variable was incorporated as an explanatory variable in the initial full model as potentially interacting with topography and/or summer precipitation anomaly (see Appendix S1). The R packages utilized to perform multiple linear regression were car (Fox & Weisberg, 2019), DHARMA (Hartig, 2020), effects (Fox & Weisberg, 2018, 2019), interactions (Long, 2019), jtools (Long, 2022), MASS (Venables & Ripley, 2002), and performance (Lüdtke et al., 2021). The significance level of all the statistical analyses performed in this study was 95% ( $\alpha=0.05$ ). For all the analyses explained in the material and methods section, data curation and visualization were performed via the tidyverse collection of R packages (Wickham et al., 2019) in R software (version 4.2.2.).

### 3 | RESULTS

The obtained results show that tree crown defoliation of holm oak across Spain has increased over the 28-year study period regardless of

the land-use type at an average rate of 0.41% year<sup>-1</sup> (Figure 3). Specifically, in 119 of the total 134 holm oak plots an increasing defoliation trend was found (i.e., Sen's slope above 0; see Figures S1 and S2). Mean annual tree crown defoliation equated to 19.43% with no differences between land uses based on the Kruskal-Wallis test results ( $p$ -value=.0669; chi-squared=3.3572; Figure 4a). However, when we look at the defoliation trends (Figure 4b), the increase rate was more acute in forests ( $n=60$ ) than in savannas ( $n=74$ ) based on the one-way ANOVA test results ( $p$ -value=.0012;  $F$  value=10.93;  $\eta^2=0.08$ ; Figure 4b).

The results of the PCA with the topographic variables showed that the first two axes (i.e., principal components, PCs) explained 51.4% of the total variance (Figure 5). The first axis (PC1) explained 29.7% of the total variance and was dominated by the slope (mean and variance), the altitude variance, and the mean of the TWI (Figure 6a), with mean slope and TWI being the highest negative and positive loadings, respectively (Figure 6b). The second axis (PC2) explained 21.7% of the total variance and the variables that contributed

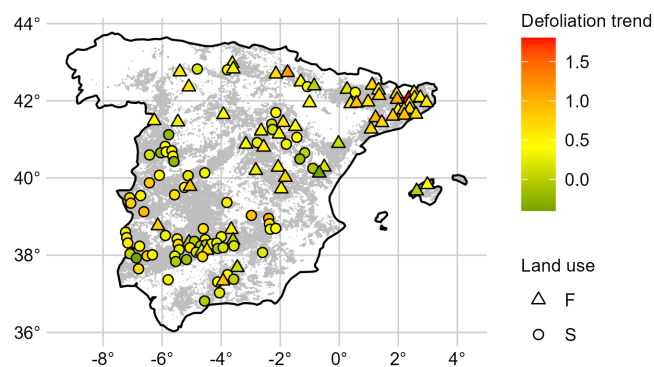


**FIGURE 3** Tree crown defoliation trend over the 1987–2014 study period (% year<sup>-1</sup> plot<sup>-1</sup>; in color) for the 134 savanna (circles) and forest (triangles) ICP holm oak plots across the distribution area of holm oak in Spain (gray area). The holm oak distribution map was provided by GIS-FOREST INIA (Ministerio de Medio Ambiente, y medio Rural y Marino, 2009). [Colour figure can be viewed at [wileyonlinelibrary.com](https://onlinelibrary.wiley.com)]

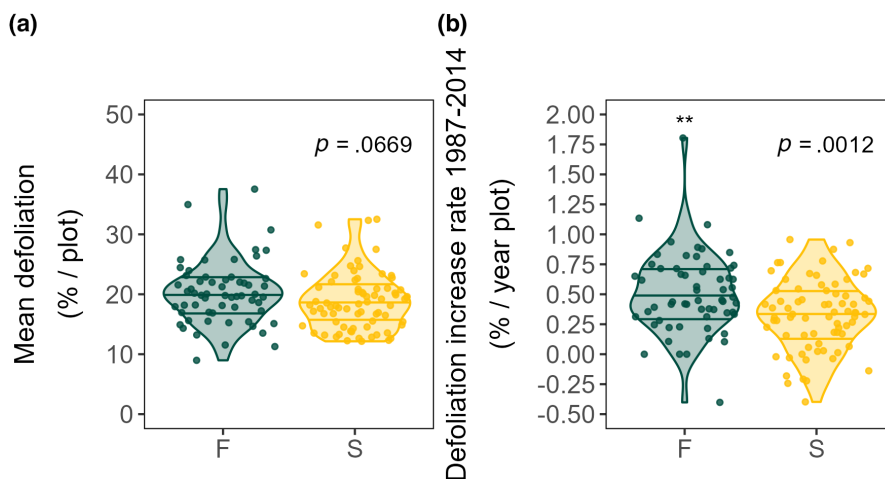


**FIGURE 4** Violin plots of (a) mean and (b) trend of crown holm oak defoliation in savannas (S; yellow;  $n=74$ ) and forests (F; green;  $n=60$ ) over the 1987–2014 period. Asterisks represent significant differences ( $p$ -value < .05) between the two land-use types. [Colour figure can be viewed at [wileyonlinelibrary.com](https://onlinelibrary.wiley.com)]

the most were: the variance of the TWI, the mean values of the planform, and the profile terrain curvatures (Figure S3). Land-use types were differently distributed only across the PC1 values. Specifically, while forests (green ellipse in Figure 5) covered the whole range of the PC1 values, savannas (yellow ellipse in Figure 5) were associated with more positive PC1 values. Overall, PCA results pointed out the link between land-use types and local topographic characteristics.

The results of Spearman correlation analyses allowed the identification of the temporally aggregated seasonal climatic anomalies that correlated the most with defoliation trends (Figure S4;  $\rho \geq 0.20$ ;  $p$ -value < .05) and did not show high correlation among them (Figure S5;  $\rho \leq 0.50$ ;  $p$ -value < .05). These climatic anomalies were the median of precipitation anomaly over the previous winter, the mean of precipitation anomaly over the previous summer, the mean of the temperature anomaly over the previous spring, and the 28-year trends of minimum and maximum temperatures over the previous summer and autumn, respectively. Hence, the annual average of the aridity index (AI) and these abovementioned climatic variables were included in the full model as well as their interactions with topography (PC1; Table S3). The selected defoliation model (Adj.  $R^2=.169$ , AIC=62.84023,  $p$ -value=.00007465) did not include coordinates as explanatory variables since residuals did not show spatial autocorrelation (Moran's I test for distance-based autocorrelation  $p$ -value=.3705). Among the predictors, only the interaction between topography (PC1) and the mean anomaly of precipitation over the previous summer showed a significant effect ( $p$ -value=.01; Table S4). However, other predictors that showed a marginal effect on defoliation trends ( $p$ -values=.05; Table S4) were the trend of the maximum temperature anomaly over the previous autumn and the interaction between topography (PC1) and the trend of the minimum temperature anomaly over the previous summer.

The model results suggest that the relationship between multidecadal trends of holm oak defoliation and the mean anomaly of precipitation over the previous summer depends on local topography (Figure 7). Those ICP plots located on steeper terrains, with

potentially lower water holding capacity (i.e., negative values of PC1), showed a negative relationship between defoliation trends and the mean anomaly of precipitation over the previous summer. Under these topographic conditions, a higher occurrence of summer droughts, depicted as negative values of the summer precipitation anomaly, was associated with higher defoliation trends. On the contrary, a positive relationship was only found for those plots with flatter topography (i.e., positive values of PC1), meaning that drier summers were related to lower defoliation trends.

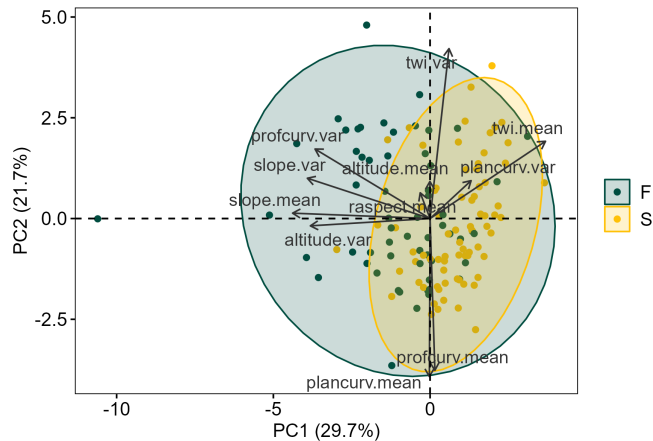


**FIGURE 5** Biplot of the principal component analysis (PCA) results for the topographic variables considered in this study, which correspond to mean (denoted as “.mean”) and variance (denoted as “.var”) values of altitude, slope, profile curvature (profcurv), planform curvature (plancurv), topographic wetness index (twi), and reclassified mean aspect (raspect.mean). Dots represent the different ICP holm oak plots with colors denoting land-use types (S, savanna in yellow and F, forest in green). Colored areas identify the general distribution of these land-use types over the first two principal components. [Colour figure can be viewed at [wileyonlinelibrary.com](http://wileyonlinelibrary.com)]

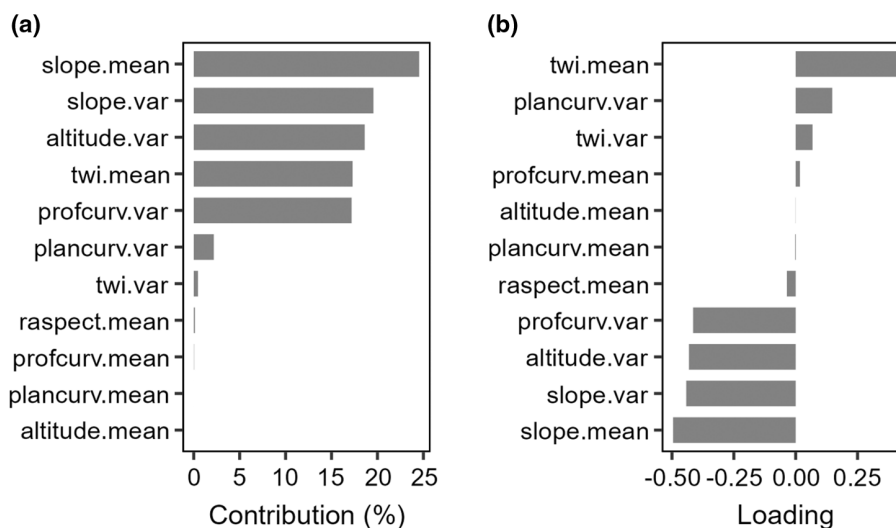


**FIGURE 6** Bar plots of the first component's (PC1) contributions (a) and loadings (b) of the 12 variables considered in the principal component analysis (PCA) which correspond to mean (denoted as “.mean”) and variance (denoted as “.var”) values of altitude, slope, profile curvature (profcurv), planform curvature (plancurv), topographic wetness index (twi), and reclassified mean aspect (raspect.mean).

## 4 | DISCUSSION

Our work proposes an approach to perform multidecadal, regional, and observational assessments of forest decline that explicitly include topography as a modulator of tree climate sensitivity. Specifically, we investigated holm oak decline in Spain from 1987 to 2014 by using crown defoliation annual surveys performed under the European ICP Forests program. These data were collected at 134 plots where the principal land-use types (forest vs. savanna) are represented, together with the topographic and climatic variability that define the area of distribution of this species within the Spanish territory. Our results show that holm oak defoliation has increased over the analyzed period being this increase rate higher in forests compared with savannas. Moreover, we have detected that the interaction between topography and summer precipitation anomalies can partially explain trends of holm oak decline in forests and savannas. While a higher occurrence of dry summers increases defoliation trends in complex terrains where forests dominate, an inverse relationship was found at flatter terrains where savannas are mainly located.

The joint influence of climate extremes, land use, and topography has hardly been considered when trying to understand holm oak decline macro-dynamics by means of any of its proxies (i.e., tree growth, defoliation, and/or mortality). However, there are few studies that evaluate the role of some of these abiotic factors separately. Regarding the effect of land use, which is used here as a term that includes both forest structure and management, Gazol et al. (2020) noticed higher holm oak growth rates in savannas compared with forests distributed across Spain. They suggest that denser stands with smaller trees are subjected to higher water competition lowering their capacity to cope with droughts or heat waves, as also proposed by Moreno and Cubera (2008). Their results support our finding of greater defoliation increase rates in

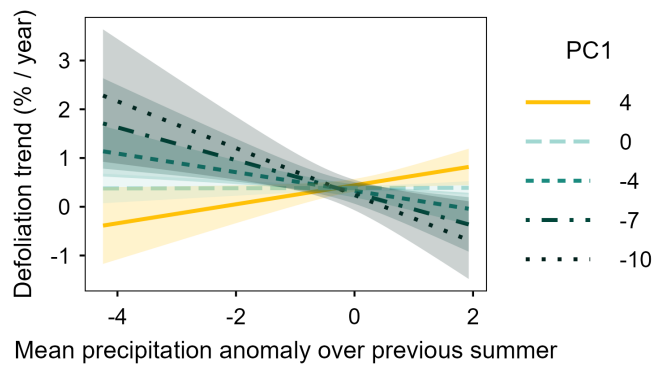


**FIGURE 7** Multiple regression model results showing the multidecadal defoliation trend as a function of the interaction between the mean precipitation anomaly over the previous summer with topography represented as PC1, with the positive and negative values representing flatter (yellow lines) and steeper terrain (green lines), respectively. Solid lines represent fitted data for the five values of PC1 represented as different colors and line types, while shaded areas correspond to the 95% confidence interval. [Colour figure can be viewed at [wileyonlinelibrary.com](https://onlinelibrary.wiley.com)]

forests compared with savannas (Figure 4). Furthermore, water stress vulnerability in holm oak forest stands has been suggested to be exacerbated by land abandonment as it promotes natural regeneration through resprouting, successional vegetation growth, and interspecific water competition (Gentilesca et al., 2017; Martínez-Vilalta et al., 2012). This reinforces the growing evidence of the suitability of forest adaptive management as a way to improve the ecosystem health and resilience against climate extremes (Domingo et al., 2020; Dwyer et al., 2007; Galiano et al., 2012; Rodríguez-Calcerrada et al., 2011).

In addition to land use, topography is a factor that should be considered to interpret the potential vulnerability of forests to climate change, especially in topographically complex areas subjected to summer drought periods as some of those covered by the area of distribution of this tree species. This is particularly relevant in the case of the Mediterranean holm oak, since topographic characteristics largely determine its forest structure and management. According to the PCA results, the land-use types considered in our study are linked to specific local topographic characteristics (Figure 5). On one hand, savannas are usually located at flatter terrains with deeper soils (Figures 5 and 6) where roots can easily access the water from deep soil layers (Moreno et al., 2005; Rolo & Moreno, 2012). On the other hand, only holm oak forests can be found at steeper areas with lower terrain-driven soil water availability (López et al., 2001). Generally, local topographic characteristics such as slope aspect and slope position are known to influence soil moisture availability in mountainous terrain (Stephenson, 1990). In this regard, previous research has demonstrated how topography can modulate vegetation responses to drought (Esteban et al., 2021; Hawthorne & Miniati, 2018; Paz-Kagan et al., 2017). These results obtained from local studies are in accordance with ours obtained regionally over three decades. Our model suggests that the most determinant factor influencing multidecadal defoliation trends was the interaction

between topography and previous summer precipitation anomaly rather than climatic variables alone (Table S4). Concretely, a higher occurrence of drier summers was related to higher defoliation increase rates only for ICP plots located at steeper terrain conditions (i.e., negative PC1 values in Figure 7), where abrupt topography (i.e., greater slopes and lower terrain-driven soil moisture) may limit soil water retention, thus amplifying water stress and thermal exposure. This topography–climate interaction could mechanistically explain our finding of greater defoliation increase rates in forests compared with savannas (Figure 4). These results are aligned with those by Galiano et al. (2012), who found a positive relationship between several decline indicators (i.e., canopy browning, and tree and stem mortality) and altitude in a holm oak forest located in NE Spain and suggested that, in this case, the negative effect of wind and radiation exposure on the ridge tops prevailed over the effect of cooler temperatures at higher altitudes.

Our study also shows how in flatter terrains, where most of the analyzed savannas are located (Figure 5), the relationship between summer precipitation anomaly and defoliation trends is completely inverse: Higher number of drier summers was related to lower defoliation increase rates in ICP plots with potentially higher topography-driven soil moisture conditions (i.e., positive values of PC1; Figure 7). Previous research primarily focused on holm oak savannas indicates no clear effect of micro-topographical features at neither local (Corcobado et al., 2013) nor regional scales (Sánchez-Cuesta et al., 2021). Regarding climate, Sánchez-Cuesta et al. (2021) identified aggregated summer SPEI over the prior 18 months and mean annual temperature as the two best predictors of holm oak annual defoliation in savannas distributed across southwestern Spain, showing negative and positive relationships, respectively, indicating that the annual defoliation and mortality of holm oak was higher in warmer and drier sites/years. Based on previous research, we suggest that this unexpected result might be explained by the fact that *Phytophthora* spp., the primary holm oak pathogen, needs soil water saturation conditions to proliferate (Gisi et al., 1980; Sterne et al., 1977). Accordingly, we found a positive relationship between tree health and dryness only for those locations more susceptible to waterlogging (i.e., higher PC1 values associated with higher TWI values; Figure 6). Indeed, a recent study based on a greenhouse experiment has shown that water stress can be beneficial for *Quercus suber* seedlings as it can reduce the *Phytophthora* spp. root damage (Homet et al., 2019). Unfortunately, it was not possible to link biotic damage information with defoliation data by using the ICP database as this was not available for the whole study period and was based purely on visual assessment. In fact, despite being the main pathogen of holm oak (Corcobado et al., 2013, 2014), *Phytophthora* spp. was not found as an identified cause of damage for any of the plots analyzed as visual diagnosis is not possible. Hence, we decided to exclude this information from our analysis to avoid making wrong conclusions based on limited information. However, several local studies have already shown the wide distribution of this pathogen and the high infection risk for holm oaks grown in the southwestern Iberian



Peninsula, where most of the savannas of our study are located (Corcobado et al., 2013, 2014; Hernández-Lambrano et al., 2018).

In order to better understand the spatiotemporal patterns of holm oak decline, future research may include spatial-explicit soil characterization data. This information must have greater spatial resolution than currently available datasets (e.g., SoilGrids) to be usable at national and regional scales, particularly on nutrients and soil texture given its link with *Phytophthora* spp. proliferation (Corcobado et al., 2013). Similarly, spatial-explicit quantitative information on forest structure (i.e., tree size, age, and density) would enhance the predictive power of our model. In this regard, although tree age may have a role in the observed defoliation patterns, we have not detected a significant effect for those plots with available data (see Appendix S1). This is probably due to the fact that tree age is provided by ICP as a discrete variable, at stand/plot spatial scale and only for the dominant tree species within each plot. Regarding tree density, the time series of European tree canopy cover initiated in 2012 (Copernicus, 2018), first with a spatial resolution of 20m and further on of 10m will become a powerful data source to include tree cover in future analysis. Furthermore, although our study has a relatively large scale, it does not cover the whole distribution area of *holm oak*, which spans from Portugal and Morocco to the Aegean Islands and western Turkey expanding northward up to northern Italy and France (de Rigo & Caudullo, 2016). International georeferenced assessments are challenging as land use, climate, and topographical maps at sufficient spatial and temporal resolutions may be in different formats, repositories or even not be publicly accessible. Nevertheless, our study builds on previous research developed at local scales that identify the main causes behind holm oak decline (*Phytophthora* spp. infestation and drought-induced decline) and sets light on spatiotemporal trends of holm oak decline for a wide range of climate, land use, and topographic conditions. Hence, our work contributes to define the “big picture” of holm oak decline as it shows, based on the categorization of decline factors developed by Manion (1981), the undeniable influence of topography and land use as predisposing factors of decline, despite being commonly neglected in regional/continental studies. Our results prove that these predisposing factors can modulate both how climate extremes (as inciting factors) affect tree health, as well as the link between these inciting factors with other contributing factors, such as pathogen infection (Gentilesca et al., 2017).

Our results are in accordance with recent research that acknowledges the outstanding role of local topography in explaining the spatial variability of forest resilience (Bramer et al., 2018; Carnicer et al., 2021; Kopecký et al., 2021; Kopecký & Čížková, 2010; Petroselli et al., 2013), as it regulates tree water availability together with thermal, radiation, and wind exposure. Overall, local stand and topographic characteristics shape forest microclimate that ultimately drives the tree response to warmer and drier climatic conditions (Zellweger et al., 2020). Finally, our findings suggest the need to adjust forest management to the local topography, closely associated with the land use and the different threats that

the Mediterranean holm oak grove faces. Thus, in topographically more complex areas where the limiting factor is water, controlling the density of trees and shrubs through thinning might help alleviate the effects of increased extreme droughts associated with climate change. On the contrary, in flatter terrains, where summer flooding can favor the proliferation of pathogens, favoring an increase in the density of trees could help to reduce the likelihood of waterlogging to limit pathogen proliferation and virulence.

## 5 | CONCLUSIONS

Contrary to previous research usually constrained to a certain region, land-use type or decline factor, our study provides a comprehensive conceptual framework to (1) investigate holm oak decline in the widest possible spectrum of uses, topography, and climate that define the distribution of this species of enormous ecological importance in the Mediterranean basin; and (2) understand, using unprecedented spatial (countrywide) and temporal (multidecadal) scales, the sensitivity of Iberian holm oaks to key abiotic factors and their interactions in space and time. Our results contribute to the incipient but growing scientific trend that acknowledges the influence of local topography on forest functioning, as it can shape forest vulnerability against climate extremes. The present work offers guidance to identify potential holm oak decline hotspots and design proper spatial-explicit measures to improve the health and future stability of Mediterranean oak ecosystems in current and future climate change scenarios. Broadly speaking, our study shows how the future forest management of holm oak stands will be key to guarantee their survival, adapting tree density to topography-dependent risks such as climate change and soil pathogens such as *Phytophthora* spp.

## ACKNOWLEDGMENTS

This work was supported by the Juan de la Cierva-Incorporación postdoctoral contract IJC2020-045630-I and the MANAGE4FUTURE project (TED2021-129499A-I00), both funded by MCIN/AEI/10.13039/501100011033 and the European Union NextGenerationEU/PRTR, the BERC 2018-2021 (Basque Government), the BC3 María de Maeztu Excellence Unit 2023-2027 Ref. CEX2021-001201-M, funded by MCIN/AEI /10.13039/501100011033 (Agencia Estatal de Investigación, Spanish Ministry of Science, and Innovation), and the Gobierno de Aragón S74\_23R research group. Ana-Maria Hereş was financed by the REASONING (PN-III-P1-1.1-TE-2019-1099) project through UEFISCDI (link; Romanian Ministry of Education and Research). This research was supported by ERC was financed by the RH2O-ARID (P18-RT-5130) project founded by the Junta de Andalucía with European Union funds for regional development and the Ramon y Cajal fellowship (RYC2020-030762-I). We acknowledge Asier Peral Beitia and Nerea Urcola Lázaro for preliminary GIS analysis, Diego Riveros-Iregui for the inspiring talks, Juan Pedro Ferrio for his useful comments, and the three anonymous reviewers whose comments substantially improved our manuscript.

## CONFLICT OF INTEREST STATEMENT

The authors declare they have no conflict of interest.

## DATA AVAILABILITY STATEMENT

Databases utilized in this study are all publicly available at the sources indicated in the material and methods and supplementary materials sections.

## ORCID

Ana López-Ballesteros  <https://orcid.org/0000-0003-0609-360X>

Emilio Rodríguez-Caballero  <https://orcid.org/0000-0002-5934-3214>

Gerardo Moreno  <https://orcid.org/0000-0001-8053-2696>

Ana-Maria Hereş  <https://orcid.org/0000-0002-1839-1770>

Jorge Curiel Yuste  <https://orcid.org/0000-0002-3221-6960>

## REFERENCES

- Adams, B. T., Matthews, S. N., Iverson, L. R., Prasad, A. M., Peters, M. P., & Zhao, K. (2021). Spring phenological variability promoted by topography and vegetation assembly processes in a temperate forest landscape. *Agricultural and Forest Meteorology*, 308–309, 108578. <https://doi.org/10.1016/J.AGRFORMET.2021.108578>
- Alfaro-Sánchez, R., Jump, A. S., Pino, J., Díez-Nogales, O., & Espelta, J. M. (2019). Land use legacies drive higher growth, lower wood density and enhanced climatic sensitivity in recently established forests. *Agricultural and Forest Meteorology*, 276–277, 107630. <https://doi.org/10.1016/J.AGRFORMET.2019.107630>
- Allen, C. D., Breshears, D. D., McDowell, N. G., Allen, C., Breshears, D. D., & McDowell, N. G. (2015). On underestimation of global vulnerability to tree mortality and forest die-off from hotter drought in the Anthropocene. *Ecosphere*, 6(8), 1–55. <https://doi.org/10.1890/ES15-00203.1>
- Allen, C. D., Macalady, A. K., Chenchouni, H., Bachelet, D., McDowell, N., Vennetier, M., Kitzberger, T., Rigling, A., Breshears, D. D., Hogg, E. H. (Ted), Gonzalez, P., Fensham, R., Zhang, Z., Castro, J., Demidova, N., Lim, J. H., Allard, G., Running, S. W., Semerci, A., & Cobb, N. (2010). A global overview of drought and heat-induced tree mortality reveals emerging climate change risks for forests. *Forest Ecology and Management*, 259(4), 660–684. <https://doi.org/10.1016/J.FORECO.2009.09.001>
- Alonso-Forn, D., Peguero-Pina, J. J., Ferrio, J. P., Mencuccini, M., Mendoza-Herrer, Ó., Sancho-Knapik, D., & Gil-Pelegrín, E. (2021). Contrasting functional strategies following severe drought in two Mediterranean oaks with different leaf habit: *Quercus faginea* and *Quercus ilex* subsp. *rotundifolia*. *Tree Physiology*, 41(3), 371–387. <https://doi.org/10.1093/TREEPHYS/TPAA135>
- Barbero, M., Loisel, R., & Quézel, P. (1992). Biogeography, ecology and history of Mediterranean *Quercus ilex* ecosystems. *Vegetatio*, 99–100(1), 19–34. <https://doi.org/10.1007/BF00118207>
- Barbeta, A., Ogaya, R., & Peñuelas, J. (2013). Dampening effects of long-term experimental drought on growth and mortality rates of a holm oak forest. *Global Change Biology*, 19(10), 3133–3144. <https://doi.org/10.1111/GCB.12269>
- Baston, D. (2022). *Exactextractr: Fast Extraction from Raster Datasets using Polygons*. R package version.9.1, <https://CRAN.R-project.org/package=exactextractr>.
- Bennie, J., Huntley, B., Wiltshire, A., Hill, M. O., & Baxter, R. (2008). Slope, aspect and climate: Spatially explicit and implicit models of topographic microclimate in chalk grassland. *Ecological Modelling*, 216(1), 47–59. <https://doi.org/10.1016/J.ECOLMODEL.2008.04.010>
- Beven, K. J., & Kirkby, M. J. (1979). A physically based, variable contributing area model of basin hydrology. *Hydrological Sciences Bulletin*, 24(1), 43–69. <https://doi.org/10.1080/02626667909491834>
- Bramer, I., Anderson, B. J., Bennie, J., Bladon, A. J., de Frenne, P., Hemming, D., Hill, R. A., Kearney, M. R., Körner, C., Korstjens, A. H., Lenoir, J., Maclean, I. M. D., Marsh, C. D., Morecroft, M. D., Ohlemüller, R., Slater, H. D., Suggitt, A. J., Zellweger, F., & Gillingham, P. K. (2018). Advances in monitoring and modelling climate at ecologically relevant scales. *Advances in Ecological Research*, 58, 101–161. <https://doi.org/10.1016/BS.AEER.2017.12.005>
- Brando, P. M., Balch, J. K., Nepstad, D. C., Morton, D. C., Putz, F. E., Coe, M. T., Silvério, D., Macedo, M. N., Davidson, E. A., Nóbrega, C. C., Alencar, A., & Soares-Filho, B. S. (2014). Abrupt increases in Amazonian tree mortality due to drought-fire interactions. *Proceedings of the National Academy of Sciences of the United States of America*, 111(17), 6347–6352. [https://doi.org/10.1073/PNAS.1305499111/SUPPL\\_FILE/PNAS.201305499SI.PDF](https://doi.org/10.1073/PNAS.1305499111/SUPPL_FILE/PNAS.201305499SI.PDF)
- Brasier, C. M. (1996). *Phytophthora cinnamomi* and oak decline in southern Europe. Environmental constraints including climate change. *Annales Des Sciences Forestières*, 53(2–3), 347–358. <https://doi.org/10.1051/FOREST:19960217>
- Brasier, C. M., Robredo, F., & Ferraz, J. F. P. (1993). Evidence for *Phytophthora cinnamomi* involvement in Iberian oak decline. *Plant Pathology*, 42(1), 140–145. <https://doi.org/10.1111/J.1365-3059.1993.TB01482.X>
- Brenning, A., Bangs, D., & Becker, M. (2018). RSAGA: SAGA geoprocessing and terrain analysis. R package version 1.3.0. <https://CRAN.R-project.org/package=RSAGA>
- Burt, T. P., & Butcher, D. P. (1985). Topographic controls of soil moisture distributions. *Journal of Soil Science*, 36(3), 469–486. <https://doi.org/10.1111/J.1365-2389.1985.TB00351.X>
- Carnicer, J., Coll, M., Ninyerola, M., Pons, X., Sánchez, G., & Peñuelas, J. (2011). Widespread crown condition decline, food web disruption, and amplified tree mortality with increased climate change-type drought. *Proceedings of the National Academy of Sciences of the United States of America*, 108(4), 1474–1478. <https://doi.org/10.1073/pnas.1010070108>
- Carnicer, J., Vives-Inglá, M., Blanquer, L., Méndez-Camps, X., Rosell, C., Sabaté, S., Gutiérrez, E., Sauras, T., Peñuelas, J., & Barbeta, A. (2021). Forest resilience to global warming is strongly modulated by local-scale topographic, microclimatic and biotic conditions. *Journal of Ecology*, 1365–2745.13752.
- Caudullo, G., Welk, E., & San-Miguel-Ayanz, J. (2017). Chorological maps for the main European woody species. *Data in Brief*, 12, 662–666. <https://doi.org/10.1016/j.dib.2017.05.007>
- Clark, K. L., Skowronski, N., & Hom, J. (2010). Invasive insects impact forest carbon dynamics. *Global Change Biology*, 16(1), 88–101. <https://doi.org/10.1111/J.1365-2486.2009.01983.X>
- Copernicus. (2018). *High resolution layer: Tree cover density (TCD) 2018. Copernicus (European Union's Earth Observation Programme)*. <https://land.copernicus.eu/pan-european/high-resolution-layer/s/forests/tree-cover-density/status-maps/tree-cover-density-2018>
- Corcobado, T., Solla, A., Madeira, M. A., & Moreno, G. (2013). Combined effects of soil properties and *Phytophthora cinnamomi* infections on *Quercus ilex* decline. *Plant and Soil*, 373(1–2), 403–413. <https://doi.org/10.1007/S11104-013-1804-Z/METRICS>
- Corcobado, T., Vivas, M., Moreno, G., & Solla, A. (2014). Ectomycorrhizal symbiosis in declining and non-declining *Quercus ilex* trees infected with or free of *Phytophthora cinnamomi*. *Forest Ecology and Management*, 324, 72–80. <https://doi.org/10.1016/J.FORECO.2014.03.040>
- Corcuera, L., Camarero, J. J., & Gil-Pelegrín, E. (2004). Effects of a severe drought on *Quercus ilex* radial growth and xylem

- anatomy. *Trees—Structure and Function*, 18(1), 83–92. <https://doi.org/10.1007/S00468-003-0284-9/FIGURES/8>
- Curiel Yuste, J., Flores-Rentería, D., García-Angulo, D., Hereş, A. M., Bragă, C., Petritan, A. M., & Petritan, I. C. (2019). Cascading effects associated with climate-change-induced conifer mortality in mountain temperate forests result in hot-spots of soil CO<sub>2</sub> emissions. *Soil Biology and Biochemistry*, 133, 50–59. <https://doi.org/10.1016/J.SOILBIO.2019.02.017>
- de Rigo, D., & Caudullo, G. (2016). *Quercus ilex* in Europe: Distribution, habitat, usage and threats. In J. San-Miguel-Ayanz, D. de Rigo, G. Caudullo, T. Houston Durrant, & A. Mauri (Eds.), *European atlas of Forest tree species* (p. e0152). Publications Office of the European Union.
- de Sampaio e Paiva Camilo-Alves, C., da Clara, M. I. E., & de Almeida Ribeiro, N. M. C. (2013). Decline of Mediterranean oak trees and its association with *Phytophthora cinnamomi*: A review. *European Journal of Forest Research*, 132(3), 411–432. <https://doi.org/10.1007/S10342-013-0688-Z>
- Domingo, J., Zavala, M. A., & Madrigal-González, J. (2020). Thinning enhances stool resistance to an extreme drought in a Mediterranean *Quercus ilex* L. coppice: Insights for adaptation. *New Forests*, 51(4), 597–613. <https://doi.org/10.1007/S11056-019-09755-4/TABLES/4>
- Douville, H., Raghavan, K., Renwick, J., Allan, R. P., Arias, P. A., Barlow, M., Cerezo-Mota, R., Cherchi, A., Gan, T. Y., Gergis, J., Jiang, D., Khan, A., Mba, W. P., Rosenfeld, D., Tierney, J., & Zolina, O. (2021). Water cycle changes. In V. Masson-Delmotte, P. Zhai, A. Pirani, S. L. Connors, C. Péan, S. Berger, N. Caud, Y. Chen, L. Goldfarb, M. I. Gomis, M. Huang, K. Leitzell, E. Lonnoy, J. B. R. Matthews, T. K. Maycock, T. Waterfield, O. Yelekçi, R. Yu, & B. Zhou (Eds.), *Climate change 2021: The physical science basis. Contribution of working group I to the sixth assessment report of the intergovernmental panel on climate change*. Cambridge University Press. In Press.
- Dwyer, J. P., Kabrick, J. M., & Wetteroff, J. (2007). Do improvement harvests mitigate oak decline in Missouri Ozark forests? *Northern Journal of Applied Forestry*, 24(2), 123–128.
- Eichhorn, J., Roskams, P., Ferretti, M., Mues, V., & Szepesi, A. (2016). *Visual assessment of crown condition and damaging agents. Manual part IV, in: Manual on methods and criteria for harmonized sampling, assessment, monitoring and analysis of the effects of air pollution on forests* (p. 49). UNECE ICP Forests Programme Co-ordinating.
- Encinas-Valero, M., Esteban, R., Hereş, A.-M., María Becerril, J., García-Plazaola, I., Artexe, U., Vivas, M., Solla, A., Moreno, G., & Yuste, J. C. (2022). Photoprotective compounds as early markers to predict holm oak crown defoliation in declining Mediterranean savannahs. *Tree Physiology*, 42(2), 208–224. <https://doi.org/10.1093/TREEPHYS/TPAB006>
- Encinas-Valero, M., Esteban, R., Hereş, A. M., Vivas, M., Fakhret, D., Aranjuelo, I., Solla, A., Moreno, G., & Curiel Yuste, J. (2022). Holm oak decline is determined by shifts in fine root phenotypic plasticity in response to belowground stress. *New Phytologist*, 235(6), 2237–2251. <https://doi.org/10.1111/NPH.18182>
- Equipo Técnico Nacional SIOSE. (2015a). *Documento Técnico SIOSE 2011*. Dirección General del Instituto Geográfico Nacional. [http://www.siose.es/SIOSEtheme-theme/documentos/pdf/Doc\\_tec\\_SIOSE\\_2011\\_v1.1.pdf](http://www.siose.es/SIOSEtheme-theme/documentos/pdf/Doc_tec_SIOSE_2011_v1.1.pdf)
- Equipo Técnico Nacional SIOSE. (2015b). *Metodología de Actualización SIOSE*. Dirección General del Instituto Geográfico Nacional. [http://www.siose.es/SIOSEtheme-theme/documentos/pdf/Method\\_Actualizacion\\_SIOSE\\_v2.pdf](http://www.siose.es/SIOSEtheme-theme/documentos/pdf/Method_Actualizacion_SIOSE_v2.pdf)
- Esteban, E. J. L., Castilho, C. V., Melgaço, K. L., & Costa, F. R. C. (2021). The other side of droughts: Wet extremes and topography as buffers of negative drought effects in an Amazonian forest. *New Phytologist*, 229(4), 1995–2006. <https://doi.org/10.1111/NPH.17005>
- Florinsky, I. V. (2000). Relationships between topographically expressed zones of flow accumulation and sites of fault intersection: Analysis by means of digital terrain modelling. *Environmental Modelling & Software*, 15(1), 87–100. [https://doi.org/10.1016/S1364-8152\(99\)00025-0](https://doi.org/10.1016/S1364-8152(99)00025-0)
- Forest Europe. (2020). *State of Europe's forests, 2020*.
- Fox, J., & Weisberg, S. (2018). Visualizing fit and lack of fit in complex regression models with predictor effect plots and partial residuals. *Journal of Statistical Software*, 87(9), 1–27. <https://www.jstatsoft.org/article/view/v087i09>
- Fox, J., & Weisberg, S. (2019). *An {R} companion to applied regression* (3rd ed.). Sage. <https://socialsciences.mcmaster.ca/jfox/Books/Companion/>
- Galiano, L., Martínez-Vilalta, J., Sabaté, S., & Lloret, F. (2012). Determinants of drought effects on crown condition and their relationship with depletion of carbon reserves in a Mediterranean holm oak forest. *Tree Physiology*, 32(4), 478–489. <https://doi.org/10.1093/TREEPHYS/TPS025>
- García-Angulo, D., Hereş, A. M., Fernández-López, M., Flores, O., Sanz, M. J., Rey, A., Valladares, F., & Curiel Yuste, J. (2020). Holm oak decline and mortality exacerbates drought effects on soil biogeochemical cycling and soil microbial communities across a climatic gradient. *Soil Biology and Biochemistry*, 149, 107921. <https://doi.org/10.1016/J.SOILBIO.2020.107921>
- García-Valdecasas Ojeda, M., Gámiz-Fortis, S. R., Romero-Jiménez, E., Rosa-Cánovas, J. J., Yeste, P., Castro-Díez, Y., & Esteban-Parra, M. J. (2021). Projected changes in the Iberian Peninsula drought characteristics. *Science of the Total Environment*, 757, 143702. <https://doi.org/10.1016/J.SCITOTENV.2020.143702>
- Gazol, A., Hereş, A.-M., & Curiel Yuste, J. (2020). Land-use practices (coppices and dehesas) and management intensity modulate responses of holm oak growth to drought. *Agricultural and Forest Meteorology*, 297, 108235. <https://doi.org/10.1016/j.agrformet.2020.108235>
- Gea-Izquierdo, G., Cherubini, P., & Cañellas, I. (2011). Tree-rings reflect the impact of climate change on *Quercus ilex* L. along a temperature gradient in Spain over the last 100 years. *Forest Ecology and Management*, 262(9), 1807–1816. <https://doi.org/10.1016/J.FORECO.2011.07.025>
- Gea-Izquierdo, G., Natalini, F., & Cardillo, E. (2021). Holm oak death is accelerated but not sudden and expresses drought legacies. *Science of the Total Environment*, 754, 141793. <https://doi.org/10.1016/J.SCITOTENV.2020.141793>
- Gentilesca, T., Camarero, J. J., Colangelo, M., Nolè, A., & Ripullone, F. (2017). Drought-induced oak decline in the western Mediterranean region: An overview on current evidences, mechanisms and management options to improve forest resilience. *IForest—Biogeosciences and Forestry*, 10(5), 796–806. <https://doi.org/10.3832/IFOR2317-010>
- Gil-Pelegrín, E., Peguero-Pina, J. J., & Sancho-Knapik, D. (2017). *Oaks and people: A long journey together* (pp. 1–11). Springer. [https://doi.org/10.1007/978-3-319-69099-5\\_1](https://doi.org/10.1007/978-3-319-69099-5_1)
- Giovannini, G., Perulli, D., Piussi, P., & Salbitano, F. (1992). Ecology of vegetative regeneration after coppicing in macchia stands in Central Italy. *Vegetatio*, 99–100(1), 331–343. <https://doi.org/10.1007/BF00118240>
- Gisi, U., Zentmyer, G. A., & Klure, L. J. (1980). Production of sporangia by *Phytophthora cinnamomi* and *P. palmivora* in soils at different matrix potentials. *Phytopathology*, 70(4), 301. <https://doi.org/10.1094/PHTO-70-301>
- González, M., Romero, M. Á., García, L. V., Gómez-Aparicio, L., & Serrano, M. S. (2020). Unravelling the role of drought as predisposing factor for *Quercus suber* decline caused by *Phytophthora cinnamomi*. *European Journal of Plant Pathology*, 156(4), 1015–1021. <https://doi.org/10.1007/S10658-020-01951-9/FIGURES/3>
- Grolemund, G., & Wickham, H. (2011). Dates and times made easy with lubridate. *Journal of Statistical Software*, 40(3), 1–25. <https://www.jstatsoft.org/v40/i03/>

- Haberstroh, S., Werner, C., Grün, M., Kreuzwieser, J., Seifert, T., Schindler, D., & Christen, A. (2022). Central European 2018 hot drought shifts scots pine forest to its tipping point. *Plant Biology*, 24(7), 1186–1197. <https://doi.org/10.1111/PLB.13455>
- Hammond, W. M., Williams, A. P., Abatzoglou, J. T., Adams, H. D., Klein, T., López, R., Sáenz-Romero, C., Hartmann, H., Breshears, D. D., & Allen, C. D. (2022). Global field observations of tree die-off reveal hotter-drought fingerprint for Earth's forests. *Nature Communications*, 13(1), 1–11. <https://doi.org/10.1038/s41467-022-29289-2>
- Harrell, F. E. (2021). *Hmisc: Harrell Miscellaneous*. R package version 4.5-0. <https://CRAN.R-project.org/package=Hmisc>.with contributions from Charles Dupont and many others
- Hartig, F. (2020). DHARMa: residual diagnostics for hierarchical (multi-level/mixed) regression models. R package version 0.3, 3(5).
- Hawthorne, S., & Miniati, C. F. (2018). Topography may mitigate drought effects on vegetation along a hillslope gradient. *Ecohydrology*, 11(1), e1825. <https://doi.org/10.1002/ECO.1825>
- Hereş, A. M., Kaye, M. W., Granda, E., Benavides, R., Lázaro-Nogal, A., Rubio-Casal, A. E., Valladares, F., & Curiel Yuste, J. (2018). Tree vigour influences secondary growth but not responsiveness to climatic variability in holm oak. *Dendrochronologia*, 49, 68–76. <https://doi.org/10.1016/J.DENDRO.2018.03.004>
- Hernández-Lambraño, R. E., González-Moreno, P., & Sánchez-Agudo, J. Á. (2018). Environmental factors associated with the spatial distribution of invasive plant pathogens in the Iberian Peninsula: The case of *Phytophthora cinnamomi* Rands. *Forest Ecology and Management*, 419–420, 101–109. <https://doi.org/10.1016/J.FORECO.2018.03.026>
- Herrera, S., Fernández, J., & Gutiérrez, J. M. (2016). Update of the Spain02 gridded observational dataset for EURO-CORDEX evaluation: Assessing the effect of the interpolation methodology. *International Journal of Climatology*, 36(2), 900–908. <https://doi.org/10.1002/joc.4391>
- Herrera, S., Gutiérrez, J. M., Ancell, R., Pons, M. R., Frías, M. D., & Fernández, J. (2012). Development and analysis of a 50-year high-resolution daily gridded precipitation dataset over Spain (Spain02). *International Journal of Climatology*, 32(1), 74–85. <https://doi.org/10.1002/joc.2256>
- Hijmans, R. J. (2021). *Raster: Geographic data analysis and modeling*. R package version 3.4-10. <https://CRAN.R-project.org/package=raster>
- Homet, P., González, M., Matías, L., Godoy, O., Pérez-Ramos, I. M., García, L. V., & Gómez-Aparicio, L. (2019). Exploring interactive effects of climate change and exotic pathogens on *Quercus suber* performance: Damage caused by *Phytophthora cinnamomi* varies across contrasting scenarios of soil moisture. *Agricultural and Forest Meteorology*, 276–277, 107605. <https://doi.org/10.1016/J.AGRFO.2019.06.004>
- Huang, Y., Chen, L., Fu, B., Huang, Z., Gong, J., & Lu, X. (2012). Effect of land use and topography on spatial variability of soil moisture in a gully catchment of the Loess Plateau, China. *Ecohydrology*, 5(6), 826–833. <https://doi.org/10.1002/ECO.273>
- Kassambara, A. (2022). *Rstatix: Pipe-friendly framework for basic statistical tests*. R package version 0.7.1 <https://CRAN.R-project.org/package=rstatix>
- Kassambara, A., & Mundt, F. (2020). *Factoextra: Extract and visualize the results of multivariate data analyses*. R package version 1.0.7. <https://CRAN.R-project.org/package=factoextra>
- Kopecký, M., & Čížková, Š. (2010). Using topographic wetness index in vegetation ecology: Does the algorithm matter? *Applied Vegetation Science*, 13(4), 450–459. <https://doi.org/10.1111/j.1654-109X.2010.01083.x>
- Kopecký, M., Macek, M., & Wild, J. (2021). Topographic wetness index calculation guidelines based on measured soil moisture and plant species composition. *Science of the Total Environment*, 757, 143785. <https://doi.org/10.1016/j.scitotenv.2020.143785>
- Lionello, P., Malanotte-Rizzoli, P., Boscolo, R., Alpert, P., Artale, V., Li, L., Luterbacher, J., May, W., Trigo, R., Tsimplis, M., Ulbrich, U., & Xoplaki, E. (2006). The Mediterranean climate: An overview of the main characteristics and issues. *Developments in Earth and Environmental Sciences*, 4(C), 1–26. [https://doi.org/10.1016/S1571-9197\(06\)80003-0](https://doi.org/10.1016/S1571-9197(06)80003-0)
- Liu, Q., Peng, C., Schneider, R., Cyr, D., McDowell, N. G., & Kneeshaw, D. (2023). Drought-induced increase in tree mortality and corresponding decrease in the carbon sink capacity of Canada's boreal forests from 1970 to 2020. *Global Change Biology*, 29, 2274–2285. <https://doi.org/10.1111/GCB.16599>
- Lloret, F., Siscart, D., & Dalmases, C. (2004). Canopy recovery after drought dieback in holm-oak Mediterranean forests of Catalonia (NE Spain). *Global Change Biology*, 10(12), 2092–2099. <https://doi.org/10.1111/J.1365-2486.2004.00870.X>
- Long, J. A. (2019). *Interactions: Comprehensive, user-friendly toolkit for probing interactions*. R package version 1.1.0, <https://cran.r-project.org/package=interactions>
- Long, J. A. (2022). *jtools: Analysis and presentation of social scientific data*. R package version 2.2.0, <https://cran.r-project.org/package=jtools>
- López, B., Sabaté, S., & Gracia, C. A. (2001). Annual and seasonal changes in fine root biomass of a *Quercus ilex* L. forest. *Plant and Soil*, 230(1), 125–134. <https://doi.org/10.1023/A:1004824719377/METRICS>
- López, B. C., Gracia, C. A., Sabaté, S., & Keenan, T. (2009). Assessing the resilience of Mediterranean holm oaks to disturbances using selective thinning. *Acta Oecologica*, 35(6), 849–854. <https://doi.org/10.1016/J.ACTAO.2009.09.001>
- Lüdecke, D., Ben-Shachar, M. S., Patil, I., Waggoner, P., & Makowski, D. (2021). Performance: An R package for assessment, comparison and testing of statistical models. *Journal of Open Source Software*, 6(60), 3139. <https://doi.org/10.21105/JOSS.03139>
- Ma, S., Concilio, A., Oakley, B., North, M., & Chen, J. (2010). Spatial variability in microclimate in a mixed-conifer forest before and after thinning and burning treatments. *Forest Ecology and Management*, 259(5), 904–915. <https://doi.org/10.1016/J.FORECO.2009.11.030>
- Manion, P. D. (1981). *Tree disease concepts*. (p. 399). Prentice-Hall, Inc.
- Markonis, Y., Kumar, R., Hanel, M., Rakovec, O., Máca, P., & Kouchak, A. A. (2021). The rise of compound warm-season droughts in Europe. *Science Advances*, 7(6), 1–7. <https://doi.org/10.1126/sciadv.abb9668>
- Martín-Sánchez, R., Peguero-Pina, J. J., Alonso-Forn, D., Ferrio, J. P., Sancho-Knapik, D., & Gil-Pelegrín, E. (2022). Summer and winter can equally stress holm oak (*Quercus ilex* L.) in Mediterranean areas: A physiological view. *Flora*, 290, 152058. <https://doi.org/10.1016/J.FLORA.2022.152058>
- Martínez-Vilalta, J., Lloret, F., & Breshears, D. D. (2012). Drought-induced forest decline: causes, scope and implications. *Biology Letters*, 8(5), 689–691. <https://doi.org/10.1098/RSBL.2011.1059>
- McDowell, N. G., Sapes, G., Pivovarov, A., Adams, H. D., Allen, C. D., Anderegg, W. R. L., Arend, M., Breshears, D. D., Brodribb, T., Choat, B., Cochard, H., de Cáceres, M., de Kauwe, M. G., Grossiord, C., Hammond, W. M., Hartmann, H., Hoch, G., Kahmen, A., Klein, T., ... Xu, C. (2022). Mechanisms of woody-plant mortality under rising drought, CO<sub>2</sub> and vapour pressure deficit. *Nature Reviews Earth & Environment*, 2022, 1–15. <https://doi.org/10.1038/s43017-022-00272-1>
- Michel, A. K., Kirchner, T., Prescher, A.-K., & Schwärzel, K. (2021). *Forest condition in Europe: The 2021 assessment*. ICP Forests Technical Report under the UNECE Convention on Long-Range Transboundary Air Pollution (Air Convention) <https://doi.org/10.3220/ICPTR1624952851000>
- Ministerio de Medio Ambiente, y Medio Rural y Marino. (2009). *Regiones de Procedencia de las Especies Forestales Españolas*. <https://sites.google.com/site/sigtreeforestspeciesenglis/home>
- Moran, P. A. P. (1950). Notes on continuous stochastic phenomena. *Biometrika*, 37(1/2), 17. <https://doi.org/10.2307/2332142>

- Moreno, G., & Cubera, E. (2008). Impact of stand density on water status and leaf gas exchange in *Quercus ilex*. *Forest Ecology and Management*, 254(1), 74–84. <https://doi.org/10.1016/J.FORECO.2007.07.029>
- Moreno, G., Obrador, J. J., Cubera, E., & Dupraz, C. (2005). Fine root distribution in Dehesas of Central-Western Spain. *Plant and Soil*, 277(1–2), 153–162. <https://doi.org/10.1007/S11104-005-6805-0/METRICS>
- Moreno, G., & Rolo, V. (2019). *Agroforestry practices: Silvopastoralism. Agroforestry for sustainable agriculture* (pp. 1–47). Burleigh Dodds Science Publishing. <https://doi.org/10.19103/AS.2018.0041.05>
- Parmesan, C., Morecroft, M. D., Trisurat, Y., Adrian, R., Anshari, G. Z., Arneth, A., Gao, Q., Gonzalez, P., Harris, R., Price, J., Stevens, N., & Talukdar, G. H. (2022). Terrestrial and freshwater ecosystems and their services. In H.-O. Pörtner, D. C. Roberts, M. Tignor, E. S. Poloczanska, K. Mintenbeck, A. Alegría, M. Craig, S. Langsdorf, S. Löschke, V. Möller, A. Okem, & B. Rama (Eds.), *Climate change 2022: Impacts, adaptation, and vulnerability. Contribution of working group II to the sixth assessment report of the intergovernmental panel on climate change*. Cambridge University Press.
- Paz-Kagan, T., Brodrick, P. G., Vaughn, N. R., Das, A. J., Stephenson, N. L., Nydick, K. R., & Asner, G. P. (2017). What mediates tree mortality during drought in the southern Sierra Nevada? *Ecological Applications*, 27(8), 2443–2457. <https://doi.org/10.1002/EAP.1620>
- Pebesma, E. (2018). Simple features for R: Standardized support for spatial vector data. *The R Journal*, 10(1), 439–446. <https://doi.org/10.32614/RJ-2018-009>
- Petrosselli, A., Vessella, F., Cavagnuolo, L., Piovesan, G., & Schirone, B. (2013). Ecological behavior of *Quercus suber* and *Quercus ilex* inferred by topographic wetness index (TWI). *Trees—Structure and Function*, 27(5), 1201–1215. <https://doi.org/10.1007/S00468-013-0869-X/TABLES/4>
- Pierce, D. (2019). *ncdf4: Interface to Unidata netCDF (version 4 or earlier) format data files*. R Package Version 1.17. <https://CRAN.R-project.org/package=ncdf4>
- Plieninger, T., Hartel, T., Martín-López, B., Beaufoy, G., Bergmeier, E., Kirby, K., Montero, M. J., Moreno, G., Oteros-Rozas, E., & Van Uytvanck, J. (2015). Wood-pastures of Europe: Geographic coverage, social-ecological values, conservation management, and policy implications. *Biological Conservation*, 190, 70–79. <https://doi.org/10.1016/J.BIOCON.2015.05.014>
- Pohlert, T. (2020). *Trend: Non-parametric trend tests and change-point detection*. R package version 1.1.4. <https://CRAN.R-project.org/package=trend>
- Pulido, F. J., Diaz, M., & Hidalgo De Trucios, S. J. (2001). Size structure and regeneration of Spanish holm oak *Quercus ilex* forests and dehesas: effects of agroforestry use on their long-term sustainability. *Forest Ecology and Management*, 146(1–3), 1–13. [https://doi.org/10.1016/S0378-1127\(00\)00443-6](https://doi.org/10.1016/S0378-1127(00)00443-6)
- Quinn, P., Beven, K., Chevallier, P., & Planchon, O. (1991). The prediction of hillslope flow paths for distributed hydrological modelling using digital terrain models. *Hydrological Processes*, 5(1), 59–79. <https://doi.org/10.1002/HYP.3360050106>
- Rodríguez, A., Curiel Yuste, J., Rey, A., Durán, J., García-Camacho, R., Gallardo, A., & Valladares, F. (2017). Holm oak decline triggers changes in plant succession and microbial communities, with implications for ecosystem C and N cycling. *Plant and Soil*, 414(1–2), 247–263. <https://doi.org/10.1007/S11104-016-3118-4/METRICS>
- Rodríguez-Calcerrada, J., Pérez-Ramos, I. M., Ourcival, J. M., Limousin, J. M., Joffre, R., & Rambal, S. (2011). Is selective thinning an adequate practice for adapting *Quercus ilex* coppices to climate change? *Annals of Forest Science*, 68(3), 575–585. <https://doi.org/10.1007/S13595-011-0050-X/FIGURES/6>
- Rodríguez-Molina, M. C., Blanco-Santos, A., Palo-Núñez, E. J., Torres-Vila, L. M., Torres-Álvarez, E., & Suárez-De-La-Cámara, M. A. (2005). Seasonal and spatial mortality patterns of holm oak seedlings in a reforested soil infected with *Phytophthora cinnamomi*. *Forest Pathology*, 35(6), 411–422. <https://doi.org/10.1111/J.1439-0329.2005.00423.X>
- Rolo, V., & Moreno, G. (2012). Interspecific competition induces asymmetrical rooting profile adjustments in shrub-encroached open oak woodlands. *Trees—Structure and Function*, 26(3), 997–1006. <https://doi.org/10.1007/S00468-012-0677-8/METRICS>
- Sáez, J. A. L., García, P. L., Merino, L. L., Cuenca, E. C., Cordero, A. G., & Gallardo, A. P. (2007). *Origen prehistórico de la dehesa en Extremadura: una perspectiva paleoambiental*.
- Sánchez-Cuesta, R., Ruiz-Gómez, F. J., Duque-Lazo, J., González-Moreno, P., & Navarro-Cerrillo, R. M. (2021). The environmental drivers influencing spatio-temporal dynamics of oak defoliation and mortality in dehesas of Southern Spain. *Forest Ecology and Management*, 485, 118946. <https://doi.org/10.1016/j.foreco.2021.118946>
- Sancho-Knapik, D., Mendoza-Herrer, Ó., Alonso-Forn, D., Saz, M. Á., Martín-Sánchez, R., dos Santos Silva, J. V., Ogee, J., Peguero-Pina, J. J., Gil-Pelegrín, E., & Ferrio, J. P. (2022). Vapor pressure deficit constrains transpiration and photosynthesis in holm oak: A comparison of three methods during summer drought. *Agricultural and Forest Meteorology*, 327, 109218. <https://doi.org/10.1016/J.AGRFO RMET.2022.109218>
- Sangüesa-Barreda, G., Camarero, J. J., Oliva, J., Montes, F., & Gazol, A. (2015). Past logging, drought and pathogens interact and contribute to forest dieback. *Agricultural and Forest Meteorology*, 208, 85–94. <https://doi.org/10.1016/J.AGRFORMET.2015.04.011>
- Scherrer, D., & Körner, C. (2010). Infra-red thermometry of alpine landscapes challenges climatic warming projections. *Global Change Biology*, 16(9), 2602–2613. <https://doi.org/10.1111/J.1365-2486.2009.02122.X>
- Seibert, J., & McGlynn, B. L. (2007). A new triangular multiple flow direction algorithm for computing upslope areas from gridded digital elevation models. *Water Resources Research*, 43(4), 4501. <https://doi.org/10.1029/2006WR005128>
- Seidl, R., Thom, D., Kautz, M., Martin-Benito, D., Peltoniemi, M., Vacchiano, G., Wild, J., Ascoli, D., Petr, M., Honkaniemi, J., Lexer, M. J., Trotsiuk, V., Mairota, P., Svoboda, M., Fabrika, M., Nagel, T. A., & Reyer, C. P. O. (2017). Forest disturbances under climate change. *Nature Climate Change*, 7(6), 395–402. <https://doi.org/10.1038/nclimate3303>
- Sen, P. K. (1968). Estimates of the regression coefficient based on Kendall's tau. *Journal of the American Statistical Association*, 63(324), 1379–1389. <https://doi.org/10.1080/01621459.1968.10480934>
- Seneviratne, S. I., Zhang, X., Adnan, M., Badi, W., Dereczynski, C., Di Luca, A., Ghosh, S., Iskandar, I., Kossin, J., Lewis, S., Otto, F., Pinto, I., Satoh, M., Vicente-Serrano, S. M., Wehner, M., & Zhou, B. (2021). Weather and climate extreme events in a changing climate. In V. Masson-Delmotte, P. Zhai, A. Pirani, S. L. Connors, C. Péan, S. Berger, N. Caud, Y. Chen, L. Goldfarb, M. I. Gomis, M. Huang, K. Leitzell, E. Lonnoy, J. B. R. Matthews, T. K. Maycock, T. Waterfield, O. Yelekçi, R. Yu, & B. Zhou (Eds.), *Climate change 2021: The physical science basis. Contribution of working group I to the sixth assessment report of the intergovernmental panel on climate change*. Cambridge University Press In Press.
- Senf, C., Buras, A., Zang, C. S., Rammig, A., & Seidl, R. (2020). Excess forest mortality is consistently linked to drought across Europe. *Nature Communications*, 11(1), 1–8. <https://doi.org/10.1038/s41467-020-19924-1>
- Serrada, R., Allué, M., & San Miguel, A. (1992). The coppice system in Spain. Current situation, state of art and major areas to be investigated. *Ann Ist Sper Selvic*, 23, 266–275. <https://www.researchgate.net/publication/2366275>

- te.net/publication/291772963\_The\_coppice\_system\_in\_Spain\_Current\_situation\_state\_of\_art\_and\_major\_areas\_to\_be\_investigated
- Serrano, M. S., Romero, M. Á., Homet, P., & Gómez-Aparicio, L. (2022). Climate change impact on the population dynamics of exotic pathogens: The case of the worldwide pathogen *Phytophthora cinnamomi*. *Agricultural and Forest Meteorology*, 322, 109002. <https://doi.org/10.1016/J.AGRFORMET.2022.109002>
- Stavi, I., Thevs, N., Welp, M., & Zdruli, P. (2022). Provisioning ecosystem services related with oak (*Quercus*) systems: A review of challenges and opportunities. *Agroforestry Systems*, 96(2), 293–313. <https://doi.org/10.1007/S10457-021-00718-3>
- Stephenson, N. L. (1990). Climatic control of vegetation distribution: The role of the water balance. *The American Naturalist*, 135(5), 649–670. <http://www.jstor.org/stable/2462028>
- Sterne, R. E., Zentmyer, G. A., & Kaufmann, M. R. (1977). The effect of matric and osmotic potential of soil on phytophthora root disease of *Persea indica*. *Phytopathology*, 77(12), 1491. <https://doi.org/10.1094/PHYTO-67-1491>
- Terradas, J. (1999). Holm oak and holm oak forests: An introduction. In F. Rodà, J. Retana, C. A. Gracia, & J. Bellot (Eds.), *Ecology of Mediterranean evergreen oak forests*. Ecological Studies (vol. 137, pp. 3–14). [https://doi.org/10.1007/978-3-642-58618-7\\_1](https://doi.org/10.1007/978-3-642-58618-7_1)
- Trabucco, A., & Zomer, R. (2019). Global aridity index and potential evapotranspiration (ETO) climate. *Database*, v2 figshare. Dataset. <https://doi.org/10.6084/m9.figshare.7504448.v3>
- Tromp-van Meerveld, H. J., & McDonnell, J. J. (2006). On the interrelations between topography, soil depth, soil moisture, transpiration rates and species distribution at the hillslope scale. *Advances in Water Resources*, 29(2), 293–310. <https://doi.org/10.1016/J.ADVWATRES.2005.02.016>
- Venables, W. N., & Ripley, B. D. (2002). *Modern applied statistics with S*. Springer. <https://doi.org/10.1007/978-0-387-21706-2>
- Vicente-Serrano, S. M., Lopez-Moreno, J. I., Beguería, S., Lorenzo-Lacruz, J., Sanchez-Lorenzo, A., García-Ruiz, J. M., Azorin-Molina, C., Morán-Tejeda, E., Revuelto, J., Trigo, R., Coelho, F., & Espejo, F. (2014). Evidence of increasing drought severity caused by temperature rise in southern Europe. *Environmental Research Letters*, 9(4), 044001. <https://doi.org/10.1088/1748-9326/9/4/044001>
- Wang, Z., Lyu, L., Liu, W., Liang, H., Huang, J., & Zhang, Q. B. (2021). Topographic patterns of forest decline as detected from tree rings and NDVI. *Catena*, 198, 105011. <https://doi.org/10.1016/j.catena.2020.105011>
- Wickham, H., Averick, M., Bryan, J., Chang, W., D'Agostino McGowan, L., François, R., Grolemund, G., Hayes, A., Henry, L., Hester, J., Kuhn, M., Lin Pedersen, T., Miller, E., Bache, S. M., Müller, K., Ooms, J., Robinson, D., Seidel, D. P., Spinu, V., ... Yutani, H. (2019). Welcome to the tidyverse. *Journal of Open Source Software*, 4(43), 1686. <https://doi.org/10.21105/joss.01686>
- Zellweger, F., de Frenne, P., Lenoir, J., Vangansbeke, P., Verheyen, K., Bernhardt-Römermann, M., Baeten, L., Hédli, R., Berki, I., Brunet, J., van Calster, H., Chudomelová, M., Decocq, G., Dirnböck, T., Durak, T., Heinken, T., Jaroszewicz, B., Kopecký, M., Máliš, F., ... Coomes, D. (2020). Forest microclimate dynamics drive plant responses to warming. *Science*, 368(6492), 772–775. [https://doi.org/10.1126/SCIENCE.ABA6880/SUPPL\\_FILE/ABA6880-ZELLWEGER-SM.PDF](https://doi.org/10.1126/SCIENCE.ABA6880/SUPPL_FILE/ABA6880-ZELLWEGER-SM.PDF)

## SUPPORTING INFORMATION

Additional supporting information can be found online in the Supporting Information section at the end of this article.

**How to cite this article:** López-Ballesteros, A., Rodríguez-Caballero, E., Moreno, G., Escribano, P., Hereş, A.-M., & Yuste, J. C. (2023). Topography modulates climate sensitivity of multidecadal trends of holm oak decline. *Global Change Biology*, 29, 6336–6349. <https://doi.org/10.1111/gcb.16927>